AMERICAN SOCIETY of
GENE & CELL
THERAPY

Ablation of Immunoproteasome β5i Subunit Suppresses Hypertensive Retinopathy by Blocking ATRAP Degradation in Mice

Shuai Wang,[1] Jing Li,[2] Tong Wang,[1] Jie Bai,[3] Yun-Long Zhang,[4] Qiu-Yue Lin,[3] Jing-min Li,[1] Qi Zhao,[1] Shu-Bin Guo,[4] and Hui-Hua Li[4]

[1]Department of Ophthalmology, Institute of Heart and Vascular Diseases, Second Affiliated Hospital of Dalian Medical University, Dalian 116027, Liaoning, China; [2]Department of Cardiology, Institute of Heart and Vascular Diseases, Second Affiliated Hospital of Dalian Medical University, Dalian 116027, Liaoning, China; [3]Department of Cardiology, Institute of Cardiovascular Diseases, First Affiliated Hospital of Dalian Medical University, Dalian 116011, Liaoning, China; [4]Department of Emergency Medicine, Beijing Chaoyang Hospital, Capital Medical University, Beijing 100020, China

Inflammation is associated with retinal diseases. Our recent data demonstrate that immunoproteasome catalytic subunit β2i contributes to angiotensin II (Ang II)-induced retinopathy in mice. Here, we investigated the role of another catalytic subunit β5i in regulating retinopathy and its underlying mechanisms. We induced a murine model of retinopathy by infusing Ang II (3,000 ng/kg/min) for 3 weeks into wild-type (WT) mice, β5i-knockout (KO) mice, or WT mice injected with either adenovirus-expressing β5i (Ad-β5i) or angiotensin II type 1 receptor (AT1R)-associated protein (Ad-ATRAP), which inhibits AT1R. The β5i expression and chymotrypsin-like activity were most significantly elevated in Ang II-infused retinas and serum from patients with hypertensive retinopathy. Moreover, Ang II infusion-induced retinopathy was markedly attenuated in β5i-KO mice but aggravated in Ad-β5i-injected mice. Accordingly, β5i KO markedly restored Ang II-induced downregulation of ATRAP and activation of AT1R downstream mediators, which was further enhanced in Ad-β5i-injected mice. Interestingly, overexpression of ATRAP significantly abrogated Ang II-induced retinopathy in Ad-β5i-injected mice. This study found that β5i promoted Ang II-induced retinopathy by promoting ATRAP degradation and activation of AT1R-mediated signals.

INTRODUCTION

Systemic elevated blood pressure (BP), which may affect ocular structure and function, has been associated with a wide range of major eye diseases.[1] Signs of hypertensive retinopathy (HR) are common, found in about 10% of the general adult non-diabetic population. Thus, high systemic BP has been regarded as a risk indicator for systemic morbidity and mortality worldwide.[2] Studies have revealed that the blood vessels of the eye are just as vulnerable to high systemic BP as are other vessels throughout the body. Systemic hypertension is strongly associated with changes in the retinal microvasculature, including retinal arteriolar narrowing, arteriovenous nicking, retinal hemorrhages, microaneurysms, and in severe cases, optic-disc and macular edema.[2,3] Increasing evidence suggests that neurohumoral

factors such as the renin-angiotensin-aldosterone system (RAAS) play pivotal roles in hypertension, not only by regulating BP but also by being involved in the pathophysiology of eye disease in hypertension. Angiotensin II (Ang II), a major effector of the RAAS, has been implicated in the regulation of vasoconstriction, intraocular pressure, cell proliferation, angiogenesis, fibrosis, inflammation, and superoxide production, all through angiotensin II type 1 receptor (AT1R).[4] Indeed, activation of AT1R has been implicated in the pathogenesis of many ocular disorders, such as diabetic retinopathy, hypoxia-induced retinopathy, and age-related macular degeneration (AMD).[5–7] However, the molecular mechanism that regulates the activation of AT1R signaling in HR remains unclear.

The 26S proteasome is a multi-enzyme complex that provides the main pathway for degradation of intracellular proteins in eukaryotic cells. It plays a critical role in regulating cellular processes, such as cell cycle, gene expression, signal transduction, and degradation of damaged and misfolded proteins.[8,9] There are two types of proteasomes: standard and inducible (also known as an immunoproteasome). The standard proteasome core particle contains three catalytic β subunits, β1, β2, and β5, which, respectively, have caspase-like, trypsin-like, and chymotrypsin-like activities. These standard subunits can be replaced in nascent proteasomes with the inducible subunits, low-molecular-weight protein 2 (LMP2 [β1i]), multicatalytic endopeptidase complex subunit (MECL [β2i]), and LMP7 (β5i), which form the core of the immunoproteasome. Upon stimulation by inflammatory cytokines such as interferon gamma (IFN-γ) and

tumor necrosis factor alpha (TNF-α), these standard β subunits can be replaced by three inducible β-subunits (also known as immunosubunits), including β1i (LMP2, proteasome subunit beta type-9 [PSMB9]), β2i (MECL-1, PSMB10), and β5i (LMP7, PSMB8). They are preferentially incorporated during proteasome assembly to form the immunoproteasome.[10,11] The immunosubunits are constitutively expressed in immune cells and induced in nonimmune cells in response to various stimuli, such as cytokines, Ang II, and optic-nerve crush (ONC).[10,12] Previous research has indicated that the immunosubunits β1i and β5i are mainly detected in the retinal inner (IPL) and outer plexiform layers (OPL), photoreceptor inner segments (ISs), and retinal pigment epithelium (RPE) cells,[13] containing ganglion cell, amacrine,[12] microglia, astrocytes,[14] endothelial cells, pericytes,[15] Müller cells, photoreceptor, and pigment epithelium cells.[13,16] The expression of these immunosubunits is markedly upregulated (approximately 4-fold) in retinal sections, such as glial cells, in response to cytotoxic T lymphocytes (CPLs)[13] and in the macula and periphery at all stages of AMD.[16] Other studies have demonstrated that the immunosubunits are involved in the regulation of retinopathy. Deficiency of the immunosubunits (either β1i alone or both β5i and β2i) attenuates ONC-induced apoptosis of RPE cells.[12] Furthermore, our recent results demonstrate that β2i knockout (KO) improves HR in mice.[17] However, whether other catalytic subunits participate in the development of Ang II-induced retinopathy and, if so, by what underlying mechanism remain to be explored.

In the present study, β5i was for the first time identified as a critical regulator of HR in mice. Our findings provide novel insights into the mechanism of Ang II-induced retinopathy by linking β5i to AT1R-associated protein (ATRAP) stability, which inhibits AT1R-mediated retinopathy, and they suggest that β5i may represent a novel therapeutic target for HR.

RESULTS

β5i Expression Was Upregulated in HR

To explore the role of immunoproteasomes in HR, we infused WT mice with a high dose of Ang II (3,000 ng/kg/min) for 3 weeks.[17] Immunoblotting showed that Ang II infusion time-dependently increased β5i proteins in the retina, compared with saline control (Figure S1C). We then analyzed proteasome activities at 3 weeks after Ang II infusion and found that chymotrypsin-like activity in retinal tissues had increased more than caspase-like and trypsin-like activity had in Ang II-treated mice compared with saline-treated mice (Figure 1A). qPCR analysis showed that among the six catalytic subunits of the proteasome, β5i was the most upregulated in the same tissues (Figure 1B), indicating that β5i contributed to the increase in chymotrypsin-like activity. Correspondingly, immunoblotting analysis confirmed the increase of β5i expression at the protein level (Figure 1C). We also observed that trypsin-like activity and β2i expression were markedly increased in Ang II-infused retinas (Figures 1B and 1C), which was consistent with our previous results.[17] Furthermore, immunohistochemistry (IHC) showed that β5i protein was mildly expressed in the ganglion cell layer (GCL), IPL, inner nuclear layer (INL), OPL, and RPE at basal condition and was remarkably

induced by Ang II in the regions of the GCL, IPL, INL, and OPL of the retinas, which contain ganglion cells, astrocytes, microglia, amacrine, endothelial cells, and pericytes (Figure 1D). These observations were consistent with previous findings.[12–17]

To verify these findings in our hypertensive human patients, we further examined chymotrypsin-like activity and β5i expression in these patients. There was no age, gender, or other confounding difference between control and patient populations (Table 1). Immunofluorescence (IF) staining revealed that the expression pattern of β5i proteins in retinas from normal control and HR patients was similar to that in the mouse retinas at baseline and after Ang II infusion (Figure 1E). Accordingly, serum β5i level and chymotrypsin-like activity were higher in patients with HR (n = 30) than in controls (n = 31; Figures 1F and 1G; Table 1). Overall, these results indicated that increased β5i expression in the retinas may play a role in the development of HR.

β5i Deficiency Improved Ang II-Induced Retinopathy

To investigate the effect of β5i on HR, we subjected WT and β5i-KO mice to Ang II for 3 weeks. We found that Ang II-induced elevation of systolic BP (SBP) in WT mice was reduced in β5i-KO mice, but we observed no statistically significant difference between the two groups (Figure S2A). Moreover, β5i-KO mice showed a significant reduction in β5i expression and chymotrypsin-like activity compared with WT controls after saline or Ang II infusion (Figure S2B). Ang II infusion markedly increased the thickness of inner retinal layers, especially the GCL, IPL, and INL in the central area, which were markedly reduced in β5i-KO mice (Figure 2A). Interestingly, Ang II infusion did not affect peripheral retinal thickness (Figure 2A).

We then examined whether β5i KO influenced inflammation and superoxide production in Ang II-infused retinas. IHC staining indicated that Ang II infusion caused more infiltration of Iba1-positive microglia/macrophages into the inner retinal layer compared with saline treatment, but this effect was markedly attenuated in β5i-KO mice (Figure 2B). Furthermore, Ang II infusion significantly induced increase of superoxide production (as indicated by dihydroethidium [DHE] staining) in the GCL and INL in WT mice, which was also suppressed in Ang II-treated β5i-KO mice (Figure 2B). Correspondingly, Ang II induced upregulation of inflammatory cytokines (*IL-1β*, *IL-6*) and NADPH oxidases *NOX1* and *NOX4* at the mRNA level in WT animals compared with saline-infused mice, whereas this increase was markedly attenuated in Ang II-treated β5i-KO retinas (Figure 2C). We observed no significant differences in these parameters between the two groups after saline infusion (Figures 2A–2C).

We next tested whether β5i KO altered retinal arteriolar structure. Fluorescence angiography showed that arteriolar narrowing (reflected by artery-to-vein ratio) and tortuosity were also significantly attenuated in β5i-KO retinas compared with WT controls after Ang II infusion (Figure 2D). Because oscillatory potentials (OPs) are a method for assessing the functional state of the retina and a sensitive indicator in mild disturbances of retinal circulation in
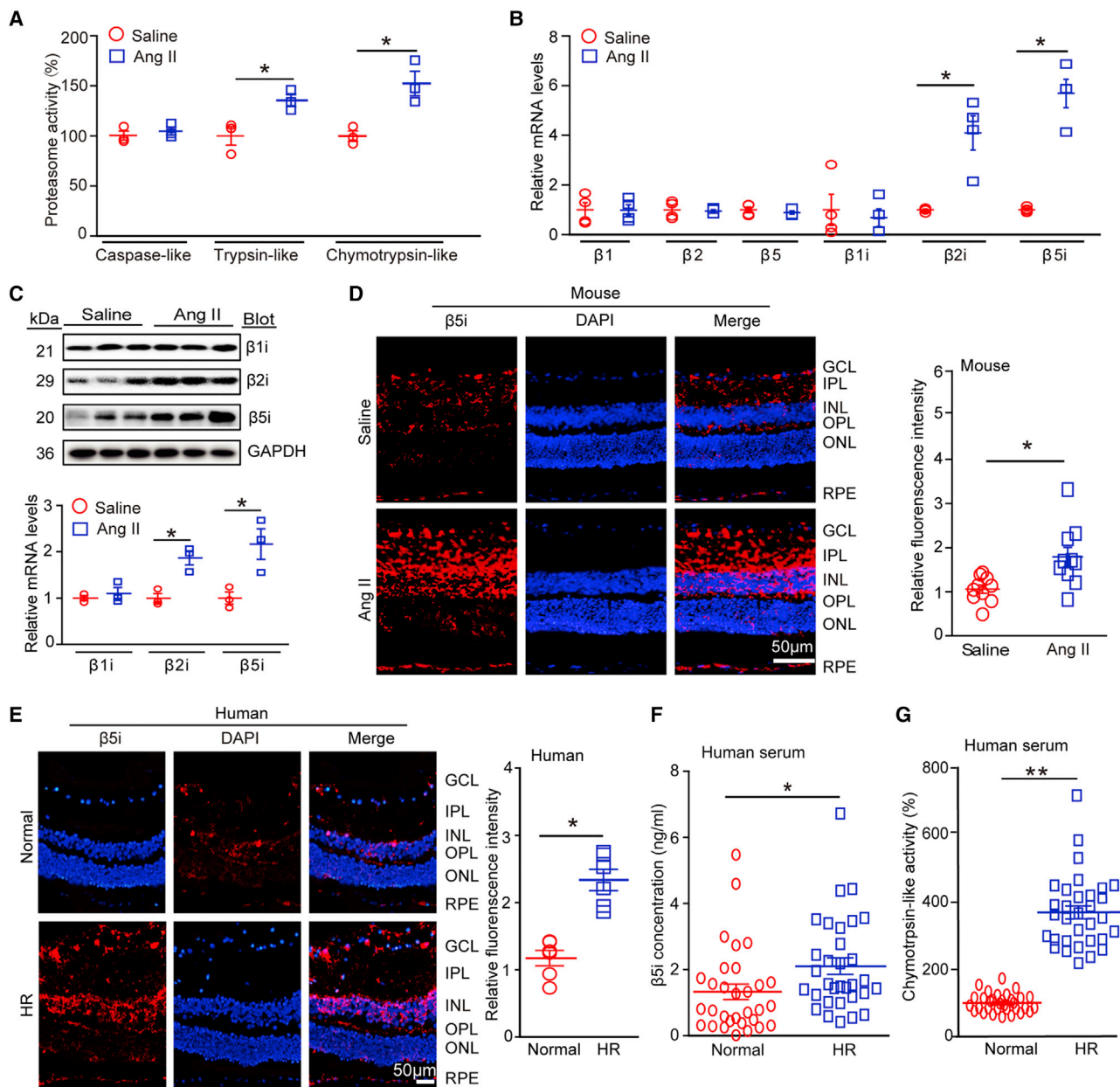
Figure 1. β5i Expression Was Upregulated in Ang II-Infused Mice and in Patients with HR

(A) WT mice were infused with Ang II at a dose of 3,000 ng/kg/min or with saline for 3 weeks. We then measured proteasome (caspase-like, trypsin-like, and chymotrypsin-like) activities in the mouse retinas (n = 3 per group). (B) qPCR analysis of expression of proteasome catalytic subunits (β1, β2, β5, β1i, β2i, and β5i) in the retinas (n = 4 per group). (C) Immunoblotting analysis of immunosubunits (β1i, β2i, and β5i; upper) and quantification of protein levels (lower; n = 3 per group). We used glyceraldehyde 3-phosphate dehydrogenase (GAPDH) as an internal control. (D) Immunostaining for β5i with anti-β5i antibody in retinal sections (left) and quantification of red fluorescence intensity (right; n = 5 per group). (E) Immunostaining for β5i antibody in retinal tissues from normal human controls and from HR patients (left), and quantification of red fluorescence intensity (right; n = 3 per group). Nuclei were counterstained with DAPI (blue). Scale bars: 50 μm. (F and G) Analysis by ELISA of β5i concentration (F) and chymotrypsin-like activity (G) in serum of controls (n = 31) and of HR patients (n = 30). Data are presented as mean ± SEM. *p < 0.05, **p < 0.01 versus saline or normal controls.

early-stage HR,[18,19] we then performed an electroretinogram (ERG). Ang II significantly decreased amplitude of OPs in WT retinas, which was reversed in Ang II-treated β5i-KO mice (Figure 2E). Because it is known that the a-wave represents photoreceptor function, whereas the b-wave represents the subsequent bipolar cell depolarization, we next measured amplitude and timing of these waves in the retinas.

Table 1. Baseline Characteristics of Normotensive Control Subjects and Hypertensive Retinopathy Patients

Parameter	Normotensive Controls (n = 31)	Hypertensive Retinopathy (n = 30)
Age (years)	53 ± 14	55 ± 12
Male (%)	59.0	61.0
Systolic blood pressure (mm Hg)	115 ± 30	154 ± 14*
Diastolic blood pressure (mm Hg)	78 ± 17	95 ± 24*
Smoke (%)	31.6	29.3
Alcohol drinking (%)	16.6	21.0
Hypertension history, years	–	13.7 ± 9.2
Hypertensive nephropathy (%)	–	11.3
Examination		
Cholesterol (mmol/L)	5.1 ± 1.2	5.1 ± 0.9
Triglycerides (mmol/L)	1.4 ± 0.4	1.6 ± 0.8
HDL (mmol/L)	1.4 ± 0.3	1.1 ± 0.6**
LDL (mmol/L)	2.9 ± 0.5	2.9 ± 0.7
Creatinemia (μmol/L)	63.1 ± 23.9	77.1 ± 29.9***
Fasting blood glucose (mmol/L)	5.2 ± 2.3	5.2 ± 0.7
White blood cell count (10^9/L)	6.1 ± 1.7	6.3 ± 2.20
Medications		
ACEI/ARB (%)	–	21.3
Beta-blocker (%)	–	50.0
Calcium channel blockers (%)	–	42.0
Statin (%)	35.5	31.3

The parameters are the mean ± SEM or n (%). ACEI, angiotensin-converting enzyme inhibitor; ARB, angiotensin receptor blocker; HDL, high-density lipoprotein; LDL, low-density lipoprotein. *p < 0.001, **p < 0.01, ***p < 0.05 versus control.

Accordingly, reduction in b-wave amplitude in Ang II-infused retinas was also markedly restored in Ang II-treated β5i-KO retinas (Figure 2E). β5i KO did not affect b-wave timing or a-wave amplitude compared with WT control after Ang II infusion (Figures S2D and S2E). There was no significant difference in OPs, amplitude, or timing of a-wave or b-wave between WT and β5i-KO mice after saline infusion (Figures 2E, S2D, and S2E), indicating that β5i KO improved Ang II-induced inner retinal dysfunction. Taken together, these results suggested that β5i deletion prevented Ang II-induced inflammation, oxidative stress, arteriolar remodeling, and retinal dysfunction in the process of retinopathy.

Increased β5i Expression Exacerbated Retinal Thickness, Inflammation, Oxidative Stress, and Arteriolar Remodeling after Ang II Infusion

To further determine whether forced β5i expression aggravated Ang II-induced retinopathy, we gave WT mice intravitreal (IVT) injections of adenovirus-expressing β5i (Ad-β5i) or adenoviruses expressing GFP (Ad-GFP) at a dose of 1.2×10^{12} plaque-forming units (PFUs)/mL and then infused them with Ang II for 3 weeks. Infection efficiency was detected by GFP fluorescence or immunostaining with

anti-β5i after injection. We found that β5i proteins were mainly expressed and colocalized with GFP in the GCL, IPL, INL, OPL, and RPE but less expressed in the retinal ONL after infection (Figure S3A). Moreover, Ang II infusion-induced elevation of SBP was further enhanced in Ad-β5i-injected mice compared with Ad-GFP-injected controls, but there was no significant difference between the two groups (Figure S3B). In addition, increases in central retinal thickness (Figure 3A); infiltration of Iba1-positive microglia/macrophages (Figure 3B); superoxide level as indicated by DHE staining (Figure 3B); arteriolar narrowing reflected by decreased artery-to-vein ratio, tortuosity, and vascular permeability (indicated by typically diffuse pale-green areas; Figure 3C); and the decrease in amplitude of OPs and b-waves in Ang II-infused retinas that Ang II infusion had induced in WT retinas were accelerated in Ad-β5i-injected mice as well (Figure 3D). Overall, these data indicated that β5i overexpression exacerbated Ang II-induced retinopathy.

β5i Activated AT1R-Mediated Signals by Targeting ATRAP Degradation

We next aimed to elucidate the mechanism by which β5i affected Ang II-induced retinopathy. Because ATRAP is reported to directly interact with and inhibit AT1R activation,[20] we examined the expression of AT1R and ATRAP in the retina. Immunostaining showed that AT1R and ATRAP proteins were mainly expressed and colocalized in the GCL, IPL, INL, OPL, and RPE at baseline (Figure S4A). The expression pattern of ATRAP was similar to that of β5i in the retinas (Figure 1D). Furthermore, immunoblotting indicated that AT1R protein levels were not significantly changed in the retina after saline or Ang II infusion (Figure 4A). However, Ang II infusion clearly reduced retinal ATRAP protein levels at 3 weeks (Figure 4A) or in a time-dependent manner (Figure S4B), rather than mRNA levels (Figure S4C), compared with saline controls. This decrease was markedly reversed in Ang II-treated β5i-KO mice (Figure 4A) but further aggravated in Ad-β5i-injected mice (Figure 4B), suggesting that β5i predominantly targeted ATRAP for degradation.

To further investigate whether β5i was directly associated with ATRAP, we performed a co-immunoprecipitation (coIP) assay in mouse retinal tissues. We found that β5i did not efficiently interact with ATRAP (Figure S4D). We then determined the location of ATRAP and β5i in the retina. Immunostaining showed that β5i was colocalized with ATRAP in the GCL, IPL, INL, OPL, and RPE after saline or Ang II infusion (Figure S4E).

To further test whether β5i modulation regulated activation of AT1R-mediated signals, we examined multiple downstream mediators of AT1R. Immunoblotting revealed that Ang II infusion activated the nuclear factor κ-light-chain-enhancer of activated B cells/p65 (NF-κB/p65), transforming growth factor beta (TGF-β)/Smad2/3, Akt, and extracellular signal-regulated kinase 1/2 (ERK1/2) signaling pathways in the retina (Figures 4C, 4D, S5A, and S5B). This activation was markedly suppressed in β5i-KO mice (Figures 4C and S5A) but enhanced in Ad-β5i-injected mice (Figures 4D and S5B). These results indicated that β5i activated
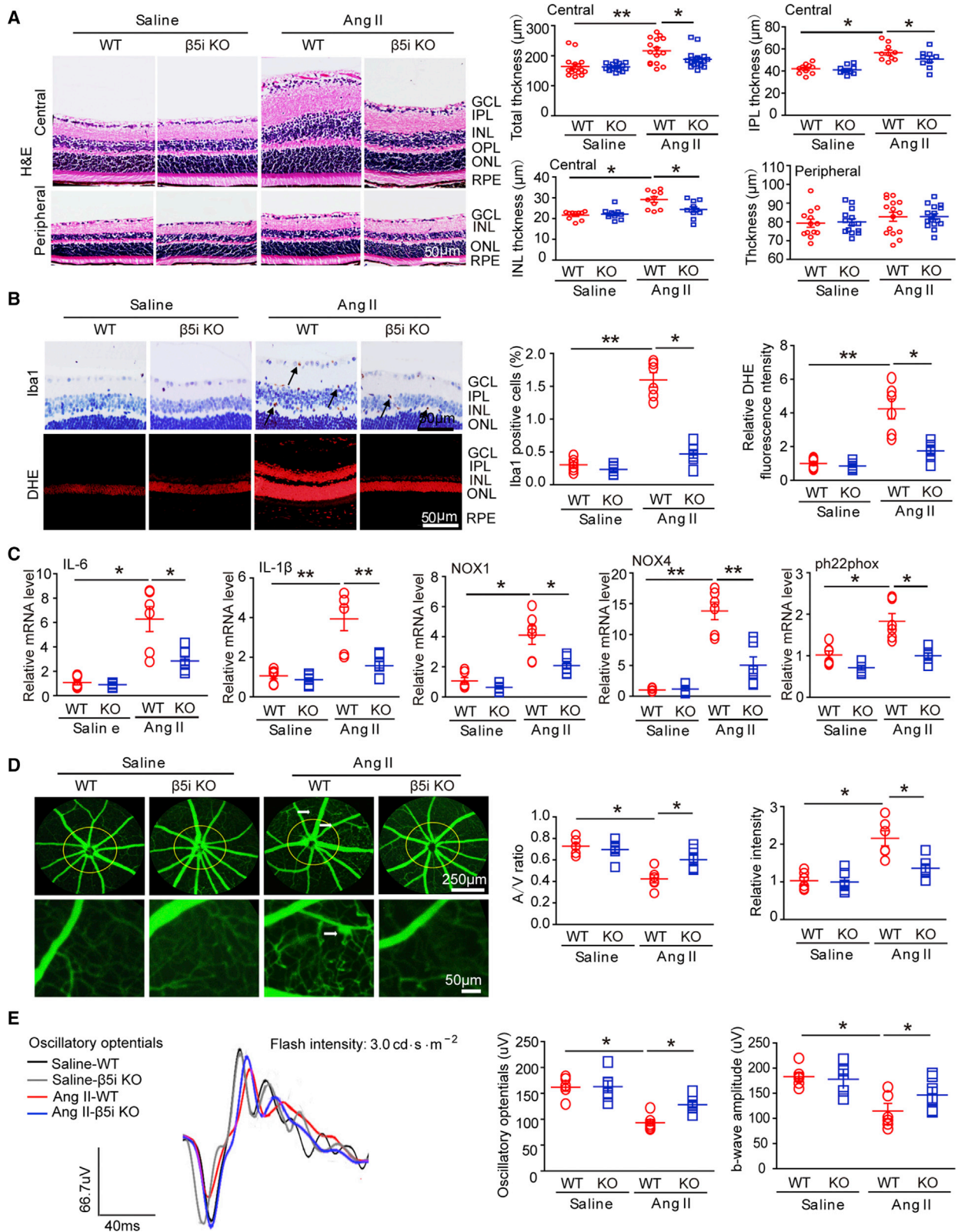
AT1R-mediated pathways by promoting ATRAP degradation in Ang II-induced retinopathy.

β5i-Enhanced Retinopathy Was Attenuated by Overexpression of ATRAP after Ang II Infusion

To specifically determine whether ATRAP was involved in β5i-mediated retinopathy induced by Ang II infusion, we injected WT mice with Ad-GFP and Ad-β5i together, with or without Ad-ATRAP, and then infused them with Ang II for 3 weeks. High infection efficiency of the retinas was achieved 3 days after adenovirus delivery. Although GFP fluorescence was strongly detected in the ONL, ATRAP proteins were mainly expressed and colocalized with GFP in the GCL, IPL, INL, and OPL (Figure S6A), which was consistent with β5i in the retinas (Figure 1D). Expression levels of Ad-β5i and Ad-ATRAP in the retinas were roughly doubled compared with Ad-GFP control after Ang II infusion (Figure 6A). Notably, local retinal Ad-ATRAP injection did not influence SBP compared with Ad-GFP injection after either saline or Ang II infusion (Figure S6B). However, ATRAP overexpression in the retinas significantly blunted Ang II-induced increases in central retinal thickness; infiltration of Iba1-positive microglia/macrophages; superoxide level as indicated by DHE staining; and arteriolar narrowing reflected by decreased artery-to-vein ratio, tortuosity, and vascular permeability (indicated by typically diffuse pale-green areas) compared with saline-treated Ad-GFP controls (Figures 5A–5C, lane 2 versus lane 1). This suggested that ATRAP played a protective role against Ang II-induced retinopathy in the mice. By contrast, overexpression of β5i accelerated Ang II-induced retinopathy (Figures 5A–5C, lane 3 versus lane 1), which was consistent with the results shown in Figure 3. As expected, ATRAP overexpression also attenuated retinopathy as indicated by increased central retinal thickness, infiltration of Iba1-positive microglia/macrophages, superoxide level, and arteriolar narrowing aggravated by Ad-β5i injection compared with Ad-GFP treatment after Ang II infusion (Figures 5A–5C, lane 4 versus lane 3). In accordance with these results, the protein levels of p-p65, TGF-β, phosphorylated ERK1/2 (p-ERK1/2), and phosphorylated Akt (p-Akt) in the retinas of Ad-GFP-injected mice were also markedly attenuated in Ad-ATRAP-injected mice after Ang II infusion (Figure 6A, lane 2 versus lane 1). Furthermore, overexpression of ATRAP reduced Ang II-induced upregulation of p-p65, TGF-β, p-ERK1/2, and p-Akt protein levels in retinas injected with Ad-β5i (Figure 6A, lane 4 versus lane 3). Overall, these results indicated that ATRAP overexpression attenuated β5i-mediated retinopathy in mice after Ang II infusion.

DISCUSSION

The present study demonstrated for the first time that immunosubunit β5i played a critical role in regulating Ang II-induced retinopathy by targeting ATRAP degradation in mice. Deletion of β5i significantly attenuated Ang II-induced retinal thickness, inflammation, oxidative stress, and retinal remodeling. Conversely, overexpression of β5i aggravated these effects. Furthermore, we found that ATRAP was a target of β5i, and that ATRAP overexpression attenuated Ang II-induced retinopathy in the setting of β5i overexpression in the retina. Mechanistically, β5i promoted ATRAP degradation, which activated AT1R-mediated signals, thereby leading to retinopathy (Figure 6B). These findings suggested that β5i may represent a therapeutic target for treating HR.

It is well documented that the primary function of the immunoproteasome is to regulate antigen presentation and immune response.[11] Increasing evidence shows that immunosubunits such as β1i and β5i are expressed in rat and human retinas, especially in the GCL, IPL, and OPL.[16,19] Moreover, the expression of such immunosubunits and relative proteasome activities are markedly upregulated in retinas and cultured RPE in response to aging and chronic oxidative stress.[21,22] Consistent with these observations, our results confirmed that β5i protein was mildly expressed in the GCL, IPL, INL, OPL, and RPE of the retinas at baseline and was remarkably induced by Ang II in these regions except RPE. Accordingly, β5i level and chymotrypsin-like activity were the most upregulated in Ang II-treated retinas and in the serum of patients with HR, compared with controls. This suggests that β5i may play a role in the development of retinal pathophysiology. Indeed, our recent results have shown that KO of β2i remarkably reduced Ang II-induced retinopathy.[17] In this study, we extended our previous findings and further demonstrated that Ang II infusion-induced retinopathy was remarkably reduced in β5i-KO mice but aggravated in β5i-overexpressing mice, suggesting that increased β5i expression efficiently promoted Ang II-induced retinopathy.

High arterial BP is linked with retinal microvascular abnormalities and prevalence of retinal-vein occlusion and retinopathy.[1,2] The RAAS is a key signaling pathway that plays an important role in regulating intraocular pressure and vasoconstriction of the retinal vascular bed through AT1R. It is well reported that the intracellular C-terminal tail of AT1R is involved in the activation of receptor-mediated signaling pathways induced by Ang II, including inflammation, oxidative stress, and production of growth factors in the process of ocular pathology.[1] Indeed, blocking AT1R activation with inhibitors has

---

Figure 2. Genetic Ablation of β5i Reduced Ang II-Induced Retinal Thickness, Inflammation, Oxidative Stress, and Vascular Dysfunction in Mice

(A) WT and β5i KO mice were infused with Ang II at a dose of 3,000 ng/kg/min or saline for 3 weeks. Representative images of H&E staining of central or peripheral retinal sections (left) and quantification of retinal thickness (right; n = 10 per group). (B) Representative images of IHC and DHE staining for Iba1 (arrows) and superoxide production, respectively, in the retinas (left). Quantification of Iba1-positive microglia/macrophages and DHE red fluorescence intensity (right; n = 6 per group). (C) qPCR analysis of IL-6, IL-1β, NOX1, NOX4, and ph22phox mRNA levels in the retinas (n = 6 per group). (D) Representative angiograms for retinal vessels (left); white arrows show perivascular fluorescein leakage. Arteriovenous ratio and quantification of fluorescence intensity (right; n = 6 per group); white arrows show perivascular fluorescein leakage. (E) Representative oscillatory potential waveforms (left) and quantification of amplitude (middle; n = 6 per group) and b-wave amplitude (right; n = 6 per group). Data are presented as mean ± SEM. *p < 0.05, **p < 0.01 versus saline controls or Ang II-infused WT mice. Scale bars: 50 or 250 μm.
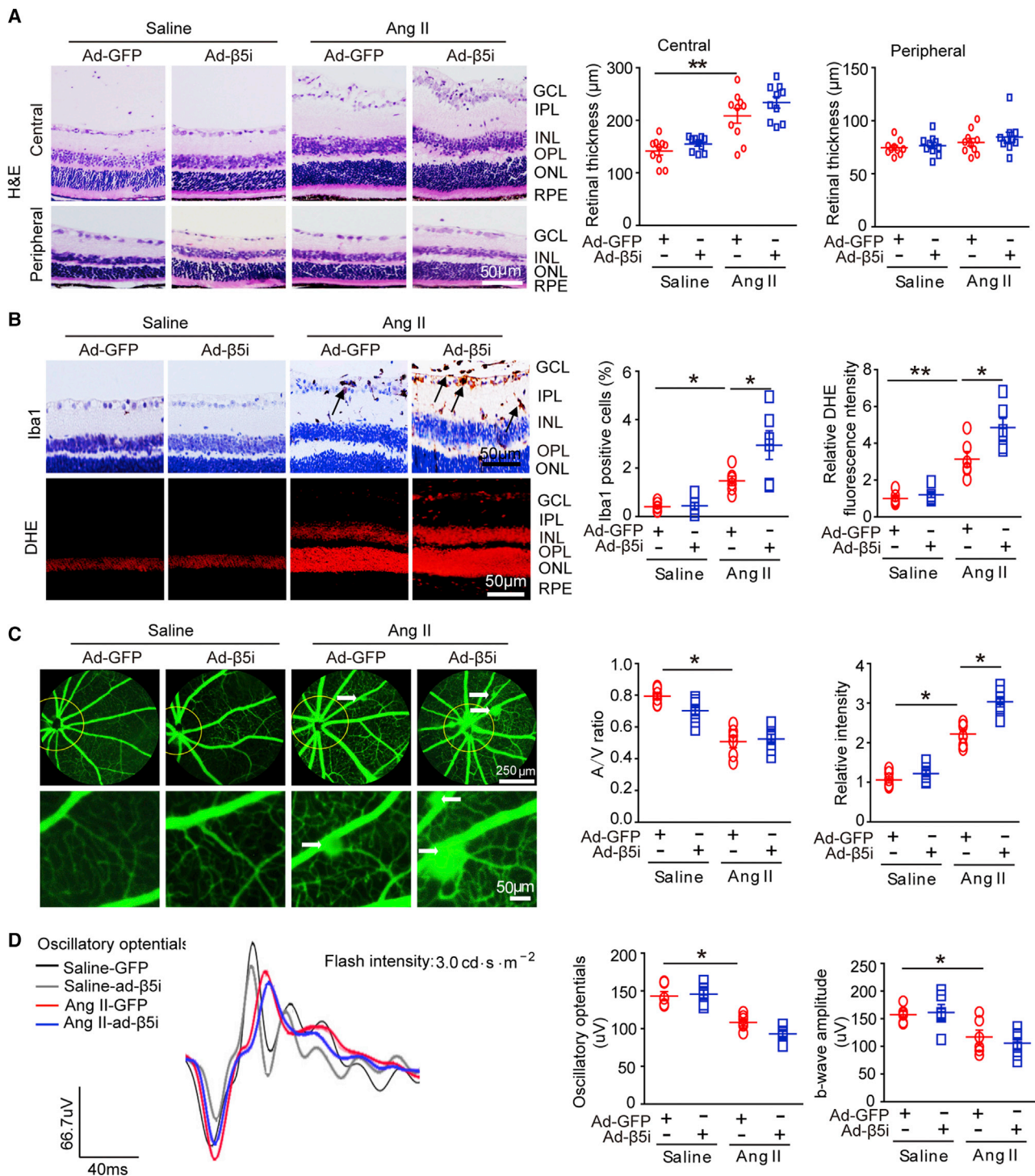
Figure 3. Overexpression of β5i Aggravated Ang II-Induced Retinopathy in Mice

(A) WT mice were locally injected with Ad-β5i or Ad-GFP at a dose of 1.2×10^{12} PFUs/mL and then infused with Ang II (3,000 ng/kg/min) for 3 weeks. Representative images of H&E staining for central or peripheral retinal sections (left) and quantification of retinal thickness (right; n = 10 per group). (B) Representative images of IHC and DHE staining
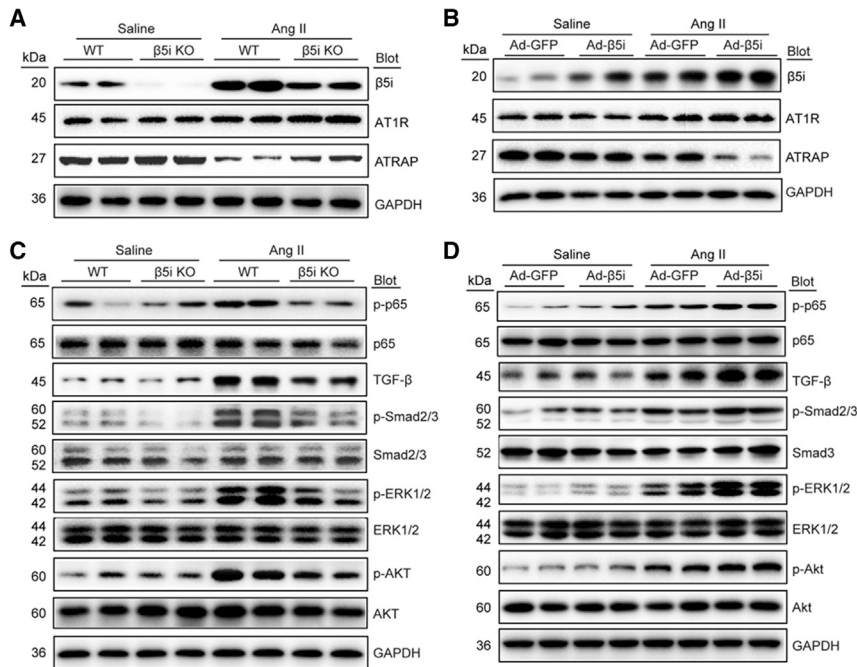
Figure 4. β5i Regulated AT1R-Mediated Downstream Signals by Targeting ATRAP Degradation

(A and C) WT and β5i KO mice were infused with Ang II at a dose of 3,000 ng/kg/min or saline for 3 weeks. Representative immunoblotting analysis of β5i, AT1R, ATRAP, p-p65, p65, TGF-β, Smad2/3, Smad3, p-Smad2/3, ERK1/2, p-ERK1/2, Akt, and p-Akt protein levels in the retinas (n = 4 per group). (B and D) WT mice were locally injected with Ad-β5i or Ad-GFP at a dose of 1.2×10^{12} PFUs/mL and then infused with Ang II (3,000 ng/kg/min) for 3 weeks. Immunoblotting analysis of the corresponding proteins in the mouse retinas was performed as in (A) (n = 4 per group). GAPDH is an internal control.

been found to improve pathology in ocular diseases such as oxygen-induced and diabetic retinopathies.[5,6] The central retinal artery and its branches supply blood to the inner retinal layers. Studies have demonstrated that Ang II-induced hypertension causes vessel hyalinization and disruption of the blood-retina barrier, which promote leakage of serum proteins and lipids into the retina, leading to fluid and blood accumulation (edema) in multiple layers of the retina.[4,23] Moreover, both inflammation and oxidative stress have been reported to play critical roles in the initiation and development of HR.[24,25] Multiple signaling pathways, including NF-κB, ROS, and TGF-β1-Smad, are known to contribute to retinopathy.[1] NF-κB signaling is a key regulator of IL-6 and ROS.[26,27] IL-6 has also been reported to induce retinal vascular inflammation and ROS activity, leading to arterial remodeling. Furthermore, amacrine cells act as intermediaries between bipolar and ganglion cells, and can transmit the visual signal to the ganglion cells. OPs are frequently used to assess amacrine cell function. Several studies suggest that AT1R has been found in the retina, particularly in Müller cells, amacrine cells, photoreceptors, the choroid, and RPE.[28,29] Interestingly, AT1R is involved in regulating the function of amacrine cells. Inflammatory cytokines such as TNF-α also induce apoptosis of amacrine cells.[30] Conversely, inhibition of AT1R by an antagonist, valsartan, protected against loss of amacrine cells in a retinopathy of prematurity rat model.[31] In this study, we showed that Ang II infusion significantly increased central retinal thickness in the GCL, IPL, and INL; inflammation; ROS production; arteriolar remodeling; and amplitude of OPs. All of these were markedly improved in β5i-KO

mice but accelerated in Ad-β5i-injected mice. Thus, our results demonstrated that upregulation of β5i enhanced Ang II-induced inflammation and oxidative stress, arteriolar remodeling, and inner retinal dysfunction, thereby leading to retinopathy in mice.

AT1R is a member of the G protein-coupled receptor (GPCR) superfamily, which mediates most of Ang II's well-known effects. Although the molecular mechanisms of AT1R regulation are not fully elucidated, several AT1R-binding proteins have been identified as inhibiting AT1R activation. Among them, ATRAP specifically interacts with the C terminus of AT1R and promotes AT1R internalization, thereby inhibiting AT1R and its downstream signals in the heart, kidneys, and vascular system.[20,32] Interestingly, our recent findings demonstrate that Ang II stimulation can induce ubiquitin-mediated degradation of ATRAP by the proteasome,[32] but whether immunoproteasomes are involved in regulating ATRAP stability remains unknown. Our current results indicated that Ang II treatment significantly reduced ATRAP levels but upregulated its downstream mediators (p65, TGF-β/Smad2/3, Akt, and ERK1/2) in the retinas of WT mice; this phenomenon was markedly reversed in β5i-KO retinas but further enhanced in Ad-β5i-injected retinas. Furthermore, increased ATRAP expression in the retinas markedly attenuated Ang II-induced inflammation, oxidative stress, and microvascular dysfunction, accompanied by reduction of downstream signals (p65, TGF-β, Akt, and ERK1/2) in Ad-β5i-injected retinas. Taken together, these results suggested that β5i promoted Ang II-induced retinopathy by mediating ATRAP degradation, which led to the activation of AT1R signaling and retinopathy upon stimulation with Ang II.

In conclusion, the present study demonstrated for the first time that β5i modulation is a regulator of HR. ATRAP is a target of

for Iba1 (arrows) and superoxide production, respectively, in the retinas (left). Quantification of Iba1-positive microglia/macrophages and DHE red intensity (right; n = 6 per group). (C) Representative angiograms for retinal vasculature; white arrows show perivascular fluorescein leakage (left). Arteriovenous ratio and quantification of fluorescence intensity (n = 6 per group). (D) Representative oscillatory potential waveforms (left) and quantification of amplitude (middle; n = 6 per group) and b-wave amplitude (right; n = 6 per group). Scale bars: 50 or 250 μm. Data are presented as mean ± SEM. *p < 0.05, **p < 0.01 versus saline control or Ang II-infused WT mice.
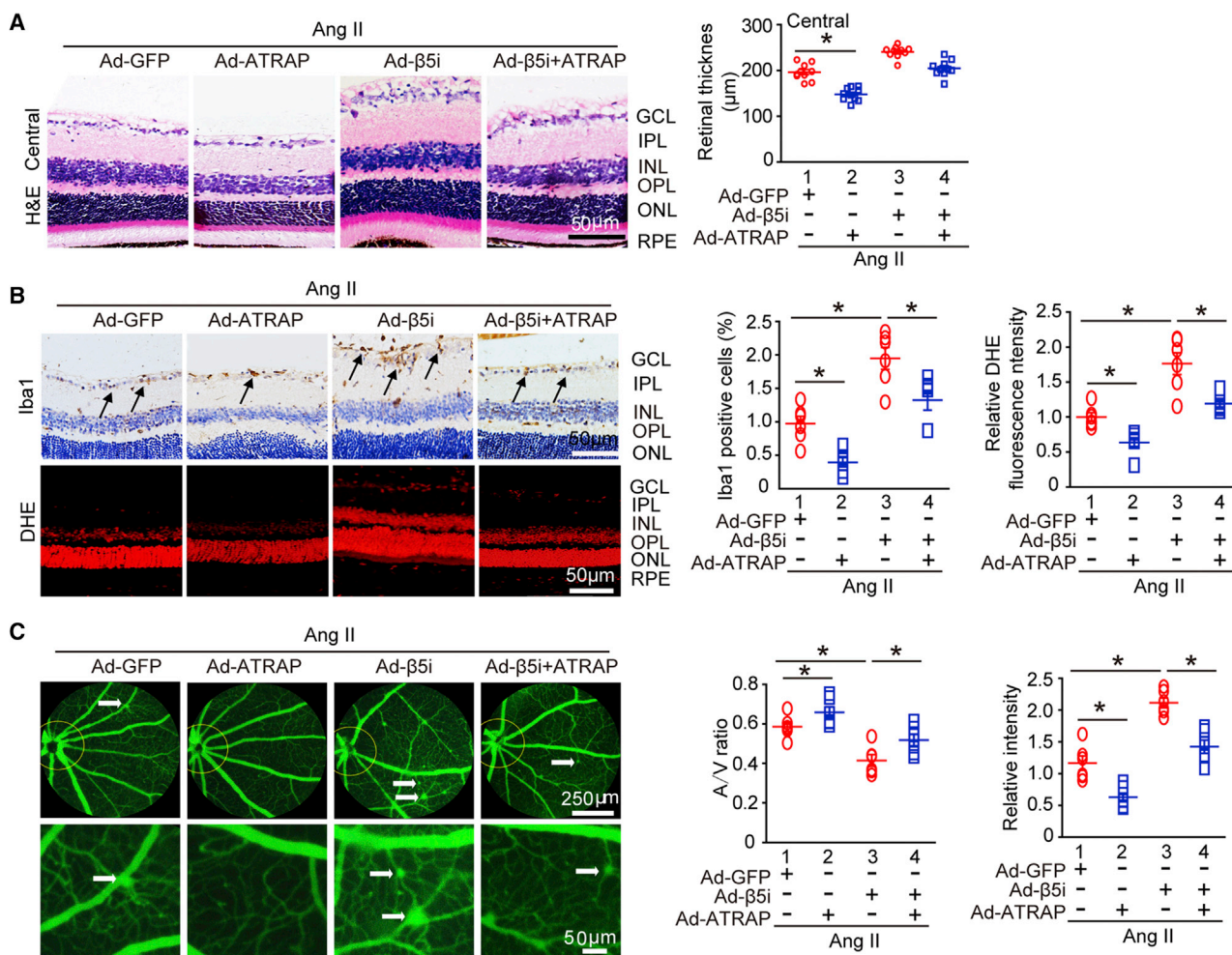
Figure 5. Increased β5i Expression Accelerated, Whereas ATRAP Blunted, Ang II-Induced Retinopathy

(A) WT mice were locally injected with Ad-β5i together with Ad-ATRAP or Ad-GFP and then infused with Ang II for 3 weeks. Representative H&E staining of the central retina (left) and quantification of retinal thickness (right; n = 10 per group). (B) Representative Iba1 and DHE staining of the central retinas (left) and quantification of Iba1-positive cells and DHE fluorescence intensity (right; n = 6 per group). (C) Representative angiograms for retinal vasculature, arteriovenous ratio, and quantification of fluorescence intensity (n = 6 per group); white arrows show perivascular fluorescein leakage. Scale bars: 50 or 250 μm. Data are presented as mean ± SEM. *p < 0.05 versus Ad-GFP-injected mice infused with Ang II or Ad-GFP+β5i-injected mice infused with Ang II.

β5i, and overexpression of ATRAP attenuated β5i and thus improved Ang II-induced retinopathy. Thus, β5i may be a potential therapeutic target for treating HR. Further studies are needed to elucidate the mechanism by which Ang II regulates β5i expression and to confirm the effect of β5i on retinopathy in other models.

MATERIALS AND METHODS

Animals and Experimental Protocols

We purchased wild-type (WT) mice and β5i-KO mice with C57BL/6 backgrounds from Jackson Laboratory (Sacramento, CA, USA) and bred them in the animal facility of Dalian Medical University (Dalian, China). All animals required 1 week of acclimatization prior to infusion. To establish a mouse model of retinop-

athy, we infused male WT and β5i-KO mice 10–12 weeks old with saline or Ang II (Sigma-Aldrich, St. Louis, MO, USA) at a dosage of 3,000 ng/kg/min using ALZET 1004 micro-osmotic pumps (DURECT, Cupertino, CA, USA) for 1–4 weeks, and then we examined histological changes and inflammatory cytokines in the retina. We found that retinal thickness and the expression of interleukin-1β and -6 (IL-1β, IL-6) were increased at weeks 1 and 2, peaked at week 3, and then slightly decreased at week 4, but there was no difference in retinal thickness or cytokine expression between weeks 3 and 4 (Figures S1A and S1B). Therefore, we infused the mice with Ang II for 3 weeks following experiments as described previously.[17] On the last day of Ang II or saline infusion, we anesthetized all mice with an intraperitoneally (i.p.) injected pentobarbital overdose (100 mg/kg; Sigma-Aldrich). We removed
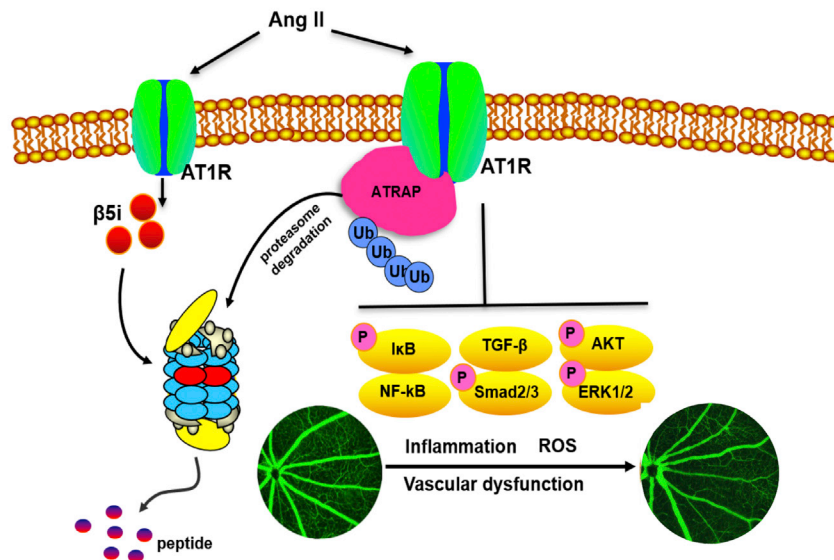
A
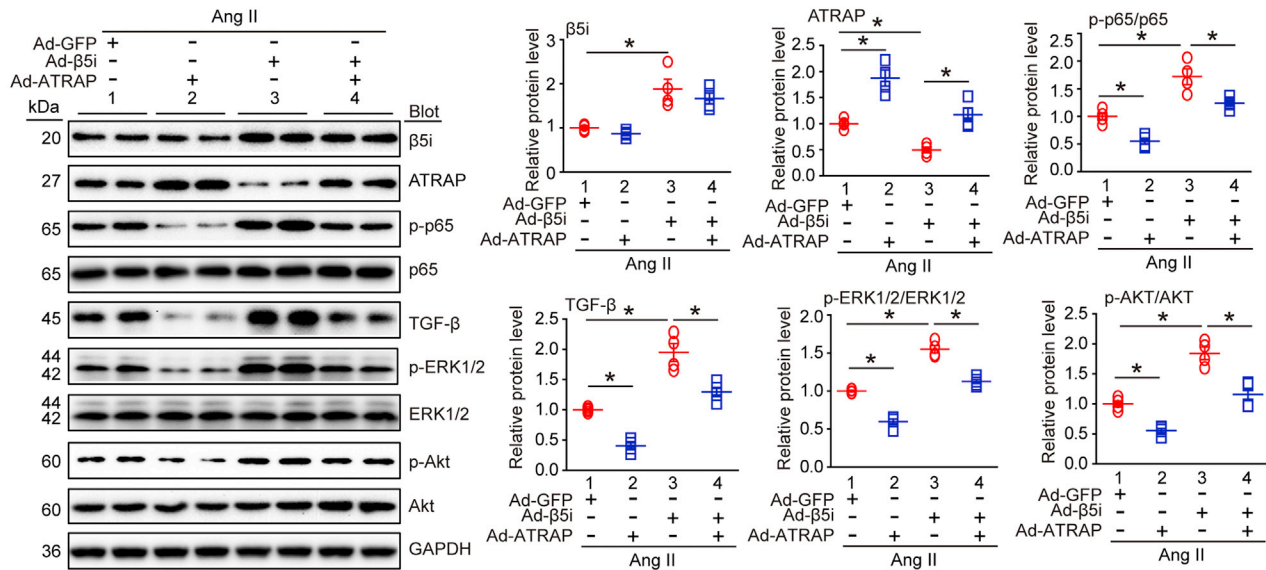
B

Figure 6. Overexpression of ATRAP Reversed β5i-Enhanced Signaling Pathways and HR after Ang II Infusion

(A) Immunoblotting analysis of β5i, ATRAP, p65, p-p65, TGF-β, ERK1/2, p-ERK1/2, Akt, and p-Akt protein expression in the retinas (left) and quantification of each protein (right; n = 4 per group). GAPDH as an internal control. Data are presented as mean ± SEM. *p < 0.05 versus Ad-GFP-injected mice infused with Ang II or Ad-β5i-injected mice infused with Ang II. (B) A working model for regulation of retinopathy by β5i. After Ang II stimulation, increased β5i expression and activity promoted ATRAP degradation, which causes activation of NF-κB-p65, TGF-β/Smad2/3, Akt, and ERK1/2 signaling pathways, thereby leading to HR.

the eyes and prepared them for further histological and molecular analysis. All animal experimentations were approved by the Institutional Animal Care and Use Committee (IACUC) of Dalian Medical University and conformed to the *Guide for the Care and Use of Laboratory Animals* as adopted by the NIH (No. 85–23; Bethesda, MD, USA).[33]

BP Recordings

We measured SBP with a BP-98A tail cuff system (Softron, Tokyo, Japan) as described previously.[34] In brief, we fastened the tail cuff with pulse transducer onto the tail bases of mice that had been placed in a plastic restrainer. A single investigator then recorded measurements in a session from 1:00 to 5:00 p.m. every 3 days.

During each session, 10 measurements were taken, and the average was used to determine the BP of each mouse.

Intravitreous Injections of Recombinant Adenoviral Vectors

We obtained recombinant adenoviruses expressing GFP (Ad-GFP), β5i (Ad-β5i), and ATRAP (Ad-ATRAP) from Hanbio (Shanghai, China). In brief, before anesthesia, mouse eyes were dilated with one compound-tropicamide eye drop (Mydrin-P; Santen Pharmaceutical, Osaka, Japan). After the pupil dilated, under a dissecting microscope, we performed intravitreal (IVT) injections using a 5-μL Hamilton microsyringe (NanoFil; World Precision Instruments, Sarasota, FL, USA) connected to a 33G needle (NF33BL-2; World Precision Instruments) as described previously.[35,36] Because the eye volume in mice is approximately 5 μL, we injected approximately 2 μL of Ad-GFP, Ad-β5i, and Ad-ATRAP at a dose of 1.2×10^{12} PFUs/mL into the IVT space of the right eye after pupillary dilation, and we repeated the injection (2 μL) in the same eye at day 3 after the first one.[36] After the injection, we applied one drop each of proparacaine 0.5% (Alcaine; Alcon, Fort Worth, TX, USA), tobramycin, and TobraDex dexamethasone ophthalmic ointment (Alcon) to the injected eye to minimize pain, risk for infection, and inflammation, respectively, in accordance with IACUC policy. We observed no significant intraocular hemorrhage, lens trauma, pressure damage, or other complications in the mice. We then evaluated the expression of Ad-GFP, Ad-β5i, and Ad-ATRAP at 3 days after the second injection (Figures S3A and S6A).

Fluorescence Angiography

We anesthetized the mice by i.p. injection of 2.5% tribromoethanol (0.020 mL/g; Sigma-Aldrich, Dorset, UK). The mice's body temperature was monitored at $37.0°C \pm 0.5°C$. Each pupil was dilated with one compound-tropicamide eye drop, and ophthalmic gel (hypromellose 2.5% ophthalmic-demulcent solution; Gonak; Akorn, Lake Forest, IL, USA) was applied to the eye. We then injected the mice with fluorescein sodium (13 mL/kg in saline; Alcon, TX, USA) via the tail vein. Afterward, we captured images of the retinal vessels using a retinal-imaging system (OPTO-RIS; Optoprobe Science, Burnaby, BC, Canada) every 30 s for 5 min. Arteries were identified by their pulsatile activity and branch anatomy. We chose a recognizable anatomical point, two optic-disc diameter from the optic disc, for each mouse to calculate an arteriovenous ratio. Measurements were compared using ImageJ software (Rasband; NIH).[37]

Electroretinography (ERG)

Mice were permitted to adapt to the dark over a period of 24 h and then anesthetized by i.p. injection of sumianxin (10%; 0.02 mL/mouse) and pentobarbital sodium (1%; 0.03 mL/kg). We desensitized the corneas of the anesthetized animals with one drop of Novesine (Novartis Ophthalmics, Basel, Switzerland) and dilated their pupils with one drop of 1% tropicamide. The animals were then placed onto a heated platform (37°C). A gold-wire electrode was placed on the corneal surface of the right eye and referenced to a gold wire in the mandible. A needle electrode in the right forelimb served as the ground. We occluded the left eye (not stimulated) with a dark patch for ERG recordings.

We performed the ERG procedure using an OPTO-III visual electrophysiology instrument (Optoprobe) as described previously.[38] Each mouse was placed into a photopic-stimulator chamber, where it was exposed to flashes of blue light once every 5–7 s. The a-wave amplitude was measured from baseline to the a-wave trough, and the b-wave amplitude was measured from the a-wave trough to the b-wave peak. OPs were measured via OP modeling. The maximum mixing reaction amplification factor of the stimulus light parameters was 4K (low frequency, 75 Hz; high frequency, 300 Hz; flash brightness, white light 600 cd·m^{-2}; flash stimulus, 5 ms; flash intensity, 3.0 cd·s·m^{-2}; and stimulus interval, 15 s). The OPs were separated from the raw ERG through 75- to 300-Hz high-pass band filtering. We measured all OP amplitudes, added them together, and averaged multiple-flash responses. The data represent the sum of OPs (OP1–OP4).

IF Staining

The eyes were fixed in 4% paraformaldehyde for 4 h at 4°C, cryopreserved overnight at 4°C in a 30% (w/v) sucrose solution, and embedded in optimal cutting temperature (OCT) medium (Leica, Wetzlar, Germany). We permeabilized the frozen sections (6 μm thick) of the eyes with 0.3% Triton X-100 in PBS for 30 min at room temperature (RT), blocked them with 3% BSA/PBS, and then incubated them at 4°C overnight with anti-β5i, AT1R (1:100; Abcam, Cambridge, MA, USA), or ATRAP (1:500 dilution; Santa Cruz, CA, USA). We then incubated the sections with secondary antibody and Alexa Fluor 594/488 (1:200) at a 1:200 dilution for 1 h and DAPI (1:10,000; Sigma, St. Louis, MO, USA) for 5 min at RT.[39] For measurement of reaction oxygen species (ROS) levels, we incubated the freshly frozen eye sections in a light-protected humidified chamber at RT with DHE (1 μM in PBS) for 30 min as described previously.[40] For intensity quantitation, we randomly selected four sections at least 60 μm apart from each eye. In each section, we captured four nonoverlapping fields at ×200 magnification using an Olympus microscope (Olympus, Tokyo, Japan) after background correction. Each microscope image collection used an identical fluorescence level. We used ImageJ software to set a threshold for immunolabeling, which we applied to all fields.

Histopathological Analysis

We anesthetized the animals with an overdose of pentobarbital sodium. The eye samples were quickly removed, fixed in 4% paraformaldehyde, embedded in paraffin, and sectioned at 5 μm. Sections were stained with H&E via the standard method. For retinal thickness measurements, we randomly selected four sections at least 60 μm apart from each eye (n = 10 per group). Central retinal thickness was measured at 500 μm off the optic-nerve head (ONH). For IHC, we incubated the sections with antibody against ionized calcium-binding adaptor molecule 1 (Iba1; 1:500; Wako, Osaka, Japan) at 4°C overnight. We used a horseradish peroxidase (HRP)-based Vectastain ABC kit (Vector Labs) with a 3,3′ diaminobenzidine (DAB) substrate to detect primary antibody. Nuclei were counterstained with hematoxylin.[40] For microglion counts, we randomly selected four sections at least 60 μm apart from each eye (n = 6 eye per group).

In each section, we captured four non-overlapping fields at ×400 magnification using the Olympus microscope after background correction. In each image region, we counted cells from the GCL to the INL using ImageJ software.

Quantitative Real-Time PCR Analysis

We extracted total RNA from the retinas using TRIzol Reagent (Invitrogen, Carlsbad, CA, USA) per the manufacturer's protocol. First-strand cDNA was synthesized from 1–2 μg total RNA by oligo (dT)-primed RT (iScript cDNA synthesis kit; Bio-Rad Laboratories, Hercules, CA, USA). We analyzed mRNA levels of *β1*, *β2*, *β5*, *β1i*, *β2i*, *β5i*, *IL-1β*, *IL-6*, nicotinamide adenine dinucleotide phosphate-oxidase 1 (*NOX1*), *NOX4*, *ph22phox*, and *ATRAP* by quantitative real-time PCR with an ABI 7500 Fast Real-Time PCR System (Applied Biosystems [Thermo Fisher Scientific, Waltham, MA, USA]). The relative levels of those genes were expressed as a ratio to that of internal control glyceraldehyde 3-phosphate dehydrogenase (GAPDH). Primers are shown in Table S1.

Western Blot Analysis

We extracted total proteins from the retinas using radioimmunoprecipitation assay (RIPA) lysis buffer (Beyotime Institute of Biotechnology, Shanghai, China) with 1% proteinase inhibitor (PMSF; Beyotime). Equal amounts of total proteins (30–40 μg) were resolved by SDS-PAGE and transferred onto polyvinylidene fluoride (PVDF) membranes, which were then incubated with ATRAP (1:500 dilution; Santa Cruz, CA, USA), AT1R, β1i, β2i, β5i (1:1,000 dilution; Abcam, Cambridge, MA, USA), and protein kinase B (Akt), p-Akt, ERK1/2, p-ERK1/2, TGF-β, Smad2/3, phosphorylated Smad2/3 (p-Smad2/3), Smad3, and GAPDH (Cell Signaling Technology [CST], Beverly, MA, USA) at 4°C overnight. We developed all blots using a FluorChem M System (ProteinSimple, CA, USA) and analyzed signal intensities with a Gel-Pro 4.5 Analyzer (Media Cybernetics, Rockville, MD, USA). Total band intensities were first normalized to GAPDH, and the ratio between phosphorylated protein and total protein was used to determine the level of signaling.

Measurement of Proteasome Activity

In brief, we purified retina proteins in 4-(2-hydroxyethyl)-1-piperazineethanesulfonic acid (HEPES) buffer (50 mM, pH 7.5) containing 20 mmol/L KCl, 5 mmol/L MgCl$_2$, and 1 mmol/L dithiothreitol (DTT). We added a total of 20 μg retinal proteins or 50 μL serum from each mouse or patient to 100 μL HEPES buffer containing the fluorogenic substrates, including Z-LLE-AMC (5 μmol/L), Ac-RLR-AMC (40 μmol/L), and Suc-LLVY-AMC (8 μmol/L; all from Promega, Fitchburg, WI, USA), and incubated the mixture at 37°C for 1 h per manufacturer's protocol. Then we measured the fluorescence intensity of each reaction using a 2030 Multilabel Microplate Reader (PerkinElmer, Waltham, MA, USA) with excitation at 380 nm and emission at 460 nm as described previously.[32]

Patients and Sample Processing

This part of the study was conducted in the Department of Cardiology, First Affiliated Hospital of Dalian Medical University between January and September 2017. All participants underwent a complete ophthalmic examination, including slit lamp microscopy and fundus examination/photography. We obtained patients' socio-demographic characteristics, drug therapy, anthropometric parameters, BP, and other relevant clinical examination data. HR patients were diagnosed according to the Keith-Wagener-Baker (KWB) as described previously.[41] Patients were not included if they had a history of intra-ocular surgery or ocular trauma; presence of a refractive power of >6.0 diopters (D) or axial length of >26.5 mm in high myopia, glaucoma, or other retinal disease; any ophthalmological diseases leading to poor fundus photographic-image quality; use of any eye drops within 3 months; or other systemic diseases (e.g., secondary hypertension, type II diabetes, sickle cell anemia, heart diseases, immune diseases, or tumor-related diseases with high chymotrypsin activity). Control subjects were defined as age- and sex-matched individuals without a history of ocular disease or any obvious abnormalities in physical or ophthalmologic examinations.

Table 1 shows the baseline characteristics of all participants (age 40–70 years). HR patients had only primary hypertension without other comorbidities. We collected serum samples from HR patients (n = 30) and age- and gender-matched normotensive healthy subjects (n = 31), and then used them to examine β5i levels or chymotrypsin-like activity with an ELISA kit (Cloud-Clone, Katy, TX, USA) per manufacturer's instructions. Human eyes were obtained within 3 h of death from six male donors (age 40–70 years) who died in road traffic accidents (three subjects with HR + three age-matched subjects without a history of ocular disease, other systemic diseases, eye injury, or fixation artifacts). A portion of each eye sample was excised, immediately fixed in 4% paraformaldehyde, and sectioned at 6 μm for immunostaining with anti-β5i antibody IF stain. The images were collected at the same location in the central retinas around 1.5 mm off the ONH. Written informed consent was obtained from each patient and control. This investigation was performed with approval by the Institutional Ethics Committee of First Affiliated Hospital of Dalian Medical University (No. LCKY2016-31). All experiments were performed in accordance with the principles outlined in the Declaration of Helsinki.

Statistical Analyses

We used SPSS software version 19.0 (SPSS, Chicago, IL, USA) to perform statistical calculations. Quantitative results are expressed as the mean ± SEM. We compared parameters using one-way ANOVA or an independent t test. $p < 0.05$ was considered to indicate a statistically significant difference.

SUPPLEMENTAL INFORMATION

Supplemental Information can be found online at https://doi.org/10.1016/j.ymthe.2019.09.025.

AUTHOR CONTRIBUTIONS

S.W. and J.L. performed research; J.L., S.W., T.W., J.B., Y.-L.Z., Q.-Y.L., J.-m.L., Q.Z., and S.-B.G. analyzed data; H.-H.L. and S.W.

conceived and designed research; H.-H.L. wrote the paper; and all authors approved the manuscript.

REFERENCES

1. Katsi, V., Marketou, M., Vlachopoulos, C., Tousoulis, D., Souretis, G., Papageorgiou, N., Stefanadis, C., Vardas, P., and Kallikazaros, I. (2012). Impact of arterial hypertension on the eye. Curr. Hypertens. Rep. 14, 581–590.

2. Bhargava, M., Ikram, M.K., and Wong, T.Y. (2012). How does hypertension affect your eyes? J. Hum. Hypertens. 26, 71–83.

3. Wong, T.Y., and Mitchell, P. (2007). The eye in hypertension. Lancet 369, 425–435.

4. Marin Garcia, P.J., and Marin-Castaño, M.E. (2014). Angiotensin II-related hypertension and eye diseases. World J. Cardiol. 6, 968–984.

5. Wilkinson-Berka, J.L. (2006). Angiotensin and diabetic retinopathy. Int. J. Biochem. Cell Biol. 38, 752–765.

6. Downie, L.E., Pianta, M.J., Vingrys, A.J., Wilkinson-Berka, J.L., and Fletcher, E.L. (2008). AT1 receptor inhibition prevents astrocyte degeneration and restores vascular growth in oxygen-induced retinopathy. Glia 56, 1076–1090.

7. Praddaude, F., Cousins, S.W., Pêcher, C., and Marin-Castaño, M.E. (2009). Angiotensin II-induced hypertension regulates AT1 receptor subtypes and extracellular matrix turnover in mouse retinal pigment epithelium. Exp. Eye Res. 89, 109–118.

8. Ferrington, D.A., and Gregerson, D.S. (2012). Immunoproteasomes: structure, function, and antigen presentation. Prog. Mol. Biol. Transl. Sci. 109, 75–112.

9. Saeki, Y., and Tanaka, K. (2012). Assembly and function of the proteasome. Methods Mol. Biol. 832, 315–337.

10. Klare, N., Seeger, M., Janek, K., Jungblut, P.R., and Dahlmann, B. (2007). Intermediate-type 20 S proteasomes in HeLa cells: "asymmetric" subunit composition, diversity and adaptation. J. Mol. Biol. 373, 1–10.

11. Angeles, A., Fung, G., and Luo, H. (2012). Immune and non-immune functions of the immunoproteasome. Front. Biosci. 17, 1904–1916.

12. Schuld, N.J., Hussong, S.A., Kapphahn, R.J., Lehmann, U., Roehrich, H., Rageh, A.A., Heuss, N.D., Bratten, W., Gregerson, D.S., and Ferrington, D.A. (2015). Immunoproteasome deficiency protects in the retina after optic nerve crush. PLoS ONE 10, e0126768.

13. Ferrington, D.A., Hussong, S.A., Roehrich, H., Kapphahn, R.J., Kavanaugh, S.M., Heuss, N.D., and Gregerson, D.S. (2008). Immunoproteasome responds to injury in the retina and brain. J. Neurochem. 106, 158–169.

14. Mishto, M., Bellavista, E., Santoro, A., Stolzing, A., Ligorio, C., Nacmias, B., Spazzafumo, L., Chiappelli, M., Licastro, F., Sorbi, S., et al. (2006). Immunoproteasome and LMP2 polymorphism in aged and Alzheimer's disease brains. Neurobiol. Aging 27, 54–66.

15. Aghdam, S.Y., Gurel, Z., Ghaffarieh, A., Sorenson, C.M., and Sheibani, N. (2013). High glucose and diabetes modulate cellular proteasome function: Implications in the pathogenesis of diabetes complications. Biochem. Biophys. Res. Commun. 432, 339–344.

16. Ethen, C.M., Hussong, S.A., Reilly, C., Feng, X., Olsen, T.W., and Ferrington, D.A. (2007). Transformation of the proteasome with age-related macular degeneration. FEBS Lett. 581, 885–890.

17. Wang, S., Li, J., Bai, J., Li, J.M., Che, Y.L., Lin, Q.Y., Zhang, Y.L., and Li, H.H. (2018). The immunoproteasome subunit LMP10 mediates angiotensin II-induced retinopathy in mice. Redox Biol. 16, 129–138.

18. Ravalico, G., Rinaldi, G., Solimano, N., Bellini, G., Cosenzi, A., Sacerdote, A., and Bocin, E. (1995). Oscillatory potentials in subjects with treated hypertension. Ophthalmologica 209, 187–189.

19. Bellini, G., Bocin, E., Cosenzi, A., Sacerdote, A., Molino, R., Solimano, N., and Ravalico, G. (1995). Oscillatory potentials of the electroretinogram in hypertensive patients. Hypertension 25, 839–841.

20. Daviet, L., Lehtonen, J.Y., Tamura, K., Griese, D.P., Horiuchi, M., and Dzau, V.J. (1999). Cloning and characterization of ATRAP, a novel protein that interacts with the angiotensin II type 1 receptor. J. Biol. Chem. 274, 17058–17062.

21. Campello, L., Esteve-Rudd, J., Cuenca, N., and Martín-Nieto, J. (2013). The ubiquitin-proteasome system in retinal health and disease. Mol. Neurobiol. 47, 790–810.

22. Hussong, S.A., Kapphahn, R.J., Phillips, S.L., Maldonado, M., and Ferrington, D.A. (2010). Immunoproteasome deficiency alters retinal proteasome's response to stress. J. Neurochem. 113, 1481–1490.

23. Fraser-Bell, S., Symes, R., and Vaze, A. (2017). Hypertensive eye disease: a review. Clin. Exp. Ophthalmol. 45, 45–53.

24. Speyer, C.L., and Ward, P.A. (2011). Role of endothelial chemokines and their receptors during inflammation. J. Invest. Surg. 24, 18–27.

25. Wang, H., and Hartnett, M.E. (2017). Roles of Nicotinamide Adenine Dinucleotide Phosphate (NADPH) Oxidase in Angiogenesis: Isoform-Specific Effects. Antioxidants 6, E40.

26. Manea, A., Tanase, L.I., Raicu, M., and Simionescu, M. (2010). Transcriptional regulation of NADPH oxidase isoforms, Nox1 and Nox4, by nuclear factor-kappaB in human aortic smooth muscle cells. Biochem. Biophys. Res. Commun. 396, 901–907.

27. Kinose, Y., Sawada, K., Makino, H., Ogura, T., Mizuno, T., Suzuki, N., Fujikawa, T., Morii, E., Nakamura, K., Sawada, I., et al. (2015). IKKβ Regulates VEGF Expression and Is a Potential Therapeutic Target for Ovarian Cancer as an Antiangiogenic Treatment. Mol. Cancer Ther. 14, 909–919.

28. Downie, L.E., Vessey, K., Miller, A., Ward, M.M., Pianta, M.J., Vingrys, A.J., Wilkinson-Berka, J.L., and Fletcher, E.L. (2009). Neuronal and glial cell expression of angiotensin II type 1 (AT1) and type 2 (AT2) receptors in the rat retina. Neuroscience 161, 195–213.

29. Milenkovic, V.M., Brockmann, M., Meyer, C., Desch, M., Schweda, F., Kurtz, A., Todorov, V., and Strauss, O. (2010). Regulation of the renin expression in the retinal pigment epithelium by systemic stimuli. Am. J. Physiol. Renal Physiol. 299, F396–F403.

30. Livne-Bar, I., Lam, S., Chan, D., Guo, X., Askar, I., Nahirnyj, A., Flanagan, J.G., and Sivak, J.M. (2016). Pharmacologic inhibition of reactive gliosis blocks TNF-α-mediated neuronal apoptosis. Cell Death Dis. 7, e2386.

31. Downie, L.E., Hatzopoulos, K.M., Pianta, M.J., Vingrys, A.J., Wilkinson-Berka, J.L., Kalloniatis, M., and Fletcher, E.L. (2010). Angiotensin type-1 receptor inhibition is neuroprotective to amacrine cells in a rat model of retinopathy of prematurity. J. Comp. Neurol. 518, 41–63.

32. Li, N., Wang, H.X., Han, Q.Y., Li, W.J., Zhang, Y.L., Du, J., Xia, Y.L., and Li, H.H. (2015). Activation of the cardiac proteasome promotes angiotension II-induced hypertrophy by down-regulation of ATRAP. J. Mol. Cell. Cardiol. 79, 303–314.

33. Kilkenny, C., Browne, W.J., Cuthill, I.C., Emerson, M., and Altman, D.G. (2010). Improving bioscience research reporting: the ARRIVE guidelines for reporting animal research. PLoS Biol. 8, e1000412.

34. Wang, L., Li, Y.L., Zhang, C.C., Cui, W., Wang, X., Xia, Y., Du, J., and Li, H.H. (2014). Inhibition of Toll-like receptor 2 reduces cardiac fibrosis by attenuating macrophage-mediated inflammation. Cardiovasc. Res. 101, 383–392.

35. Petrs-Silva, H., Dinculescu, A., Li, Q., Deng, W.T., Pang, J.J., Min, S.H., Chiodo, V., Neeley, A.W., Govindasamy, L., Bennett, A., et al. (2011). Novel properties of tyrosine-mutant AAV2 vectors in the mouse retina. Mol. Ther. 19, 293–301.

36. Hamilton, M.M., Brough, D.E., McVey, D., Bruder, J.T., King, C.R., and Wei, L.L. (2006). Repeated administration of adenovector in the eye results in efficient gene delivery. Invest. Ophthalmol. Vis. Sci. *47*, 299–305.

37. Tawfik, A., Markand, S., Al-Shabrawey, M., Mayo, J.N., Reynolds, J., Bearden, S.E., Ganapathy, V., and Smith, S.B. (2014). Alterations of retinal vasculature in cystathionine-β-synthase heterozygous mice: a model of mild to moderate hyperhomocysteinemia. Am. J. Pathol. *184*, 2573–2585.

38. Hussong, S.A., Roehrich, H., Kapphahn, R.J., Maldonado, M., Pardue, M.T., and Ferrington, D.A. (2011). A novel role for the immunoproteasome in retinal function. Invest. Ophthalmol. Vis. Sci. *52*, 714–723.

39. McGill, T.J., Prusky, G.T., Luna, G., LaVail, M.M., Fisher, S.K., and Lewis, G.P. (2012). Optomotor and immunohistochemical changes in the juvenile S334ter rat. Exp. Eye Res. *104*, 65–73.

40. Wilkinson-Berka, J.L., Deliyanti, D., Rana, I., Miller, A.G., Agrotis, A., Armani, R., Szyndralewiez, C., Wingler, K., Touyz, R.M., Cooper, M.E., et al. (2014). NADPH oxidase, NOX1, mediates vascular injury in ischemic retinopathy. Antioxid. Redox Signal. *20*, 2726–2740.

41. Keith, N.M., Wagener, H.P., and Barker, N.W. (1974). Some different types of essential hypertension: their course and prognosis. Am. J. Med. Sci. *268*, 336–345.